ELSEVIER

Int. J. Therm. Sci. 41 (2002) 201–205

International Journal of Thermal Sciences

Powers and efficiency performance of an endoreversible Braysson cycle

Junlin Zheng [a], Lingen Chen [a,*], Fengrui Sun [a], Chih Wu [b]

[a] *Faculty 306, Naval University of Engineering, Wuhan 430033, People's Republic of China*
[b] *Mechanical Engineering Department, U. S. Naval Academy, Annapolis, MD 21402, USA*

Received 28 June 2000; accepted 8 March 2001

Abstract

Performance analysis of a Braysson cycle has been performed using entropy generation minimization or finite time thermodynamics. The analytical formula about power output and efficiency of an endoreversible Braysson cycle with heat resistance losses in the hot and cold-side heat exchangers are derived. The influences of the design parameters on the performance of the cycle are analyzed by detailed numerical examples. © 2002 Éditions scientifiques et médicales Elsevier SAS. All rights reserved.

Keywords: Braysson cycle; Finite time thermodynamics; Entropy generation minimization; Power; Efficiency; Optimal performance

1. Introduction

Recently, a hybrid gas turbine cycle, Braysson cycle, has been proposed by Frost et al. [1] based on the conventional Brayton cycle for the high-temperature heat addition process while adopting the Ericsson cycle for the low-temperature heat rejection process. The First Law analysis for the Braysson cycle has been performed in Ref. [1]. The theory of entropy generation minimization or finite time thermodynamics [2–5] is a powerful tool for the engineering cycle analysis. Some authors have analyzed endoreversible Brayton [6–13] and Ericsson [14–16] performance using this theory. The objective of this paper is to study the Braysson cycle performance using this new and active theory. The analytical formula about the power output and efficiency of an endoreversible Braysson cycle with the heat resistance losses in the hot- and cold-side heat exchangers are derived. Detailed numerical examples are given in order to analyze the influences of the design parameters on the performance of the cycle.

2. Cycle analysis

An endoreversible Braysson cycle operating between a heat source at temperature T_H and a heat sink at temperature T_L with the heat resistance losses is shown in Fig. 1. The processes 4-1 and 2-3 are isentropic processes. Process 1-2 is an isobaric process. Process 3-4 is an isothermal process. There are finite temperature difference between heat source T_H and process 1-2, as well as between process 3-4 and heat sink T_L because of the heat resistance losses in the hot- and cold-side heat exchangers.

Assuming the heat exchangers are counter-flow configuration, the heat conductances (heat transfer coefficient and surface area product) of the hot- and cold-side heat exchangers are U_H and U_L, and the cycled working fluid has thermal capacitance rate C_{wf} (mass flow rate and isobaric specific heat product). Therefore, the rate of heat (Q_H) absorbed from the heat source T_H and the rate of heat (Q_L) released to the heat sink T_L are as follows from the heat exchanger theory:

$$Q_H = C_{wf} E_H (T_H - T_1) \tag{1}$$

$$Q_L = U_L (T_3 - T_L) \tag{2}$$

where E_H is the effectiveness of the hot-side heat exchanger,

$$E_H = 1 - \exp(-N_H) \tag{3}$$

* Correspondence and reprints.
E-mail addresses: lgchenna@public.wh.hb.cn (L. Chen), wu@gwmail.usna.edu (C. Wu).

1290-0729/02/$ – see front matter
PII: S1290-0729(01)01298-4

Nomenclature

C_{wf}	thermal capacitance rate of the working fluid	$W \cdot K^{-1}$	
C_p	specific heat at constant pressure	$W \cdot s \cdot K^{-1} \cdot kg^{-1}$	
E	effectiveness of the heat exchanger		
F	surface area of the heat exchanger	m^2	
m	mass flow rate of the working fluid	$kg \cdot s^{-1}$	
N	number of heat transfer units		
P	dimensionless power output		
Q	rate of heat transfer	W	
T	temperature	K	
U	heat conductance of the heat exchanger	$W \cdot K^{-1}$	
W	power output	W	
x	working fluid temperature ratio		

Greek symbols

τ	heat reservoir temperature ratio
η	thermal efficiency of the cycle

Subscripts

H	hot-side
L	cold-side
max	maximum
opt	optimum
P	at maximum power output
T	total
1, 2, 3, 4	points in the T-s diagram of the cycle

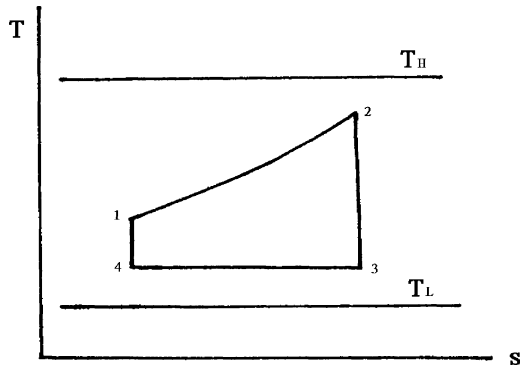

Fig. 1. T-s diagram of an endoreversible Braysson cycle.

where N_H is the number of heat transfer unit

$$N_H = U_H / C_{wf} \tag{4}$$

From the working fluid property

$$Q_H = C_{wf}(T_2 - T_1) \tag{5}$$

The power output (W) and efficiency (η) of the cycle are

$$W = Q_H - Q_L = C_{wf} E_H (T_H - T_1) - U_L (T_3 - T_L) \tag{6}$$

$$\eta = 1 - Q_L / Q_H = 1 - U_L (T_3 - T_L) / \left[C_{wf} E_H (T_H - T_1) \right] \tag{7}$$

Applying the Second Law of Thermodynamics to the cycle and the hypothesis of the perfect gas,

$$U_L (T_3 - T_L) / T_3 = m C_P \ln(T_2 / T_1) = C_{wf} \ln(T_2 / T_1) \tag{8}$$

where m is the working fluid mass flow rate.

Defining a dimensionless parameter x (dimensionless working fluid temperature ratio)

$$x = U_L (T_3 - T_L) / (C_{wf} T_3) = \ln(T_2 / T_1) \tag{9}$$

Rearranging Eq. (9) gives

$$T_3 = U_L T_L / (U_L - C_{wf} x) \tag{10}$$

$$T_2 = T_1 \exp(x) \tag{11}$$

Combining Eqs. (1) and (5) gives

$$T_2 = (1 - E_H) T_1 + E_H T_H \tag{12}$$

Combing Eqs. (11) and (12) gives

$$T_1 = E_H T_H / \left[\exp(x) + E_H - 1 \right] \tag{13}$$

$$T_2 = E_H T_H \exp(x) / \left[\exp(x) + E_H - 1 \right] \tag{14}$$

Substituting Eqs. (10), (13) and (14) into Eqs. (6) and (7) yields the dimensionless power output [$P = W/(C_{wf} T_L)$] and thermal efficiency (η) of the cycle

$$P = E_H \tau \left(e^x - 1 \right) / \left(e^x + E_H - 1 \right) - U_L x / (U_L - C_{wf} x) \tag{15}$$

$$\eta = 1 - U_L x \left(e^x + E_H - 1 \right) / \left[E_H \tau (U_L - C_{wf} x) \left(e^x - 1 \right) \right] \tag{16}$$

where $\tau = T_H / T_L$ is the heat reservoir temperature ratio of the cycle.

Eqs. (15) and (16) are the major results of this paper. They determine the relationships between the dimensionless power output and dimensionless working fluid temperature ratio, as well as between efficiency and dimensionless working fluid temperature ratio. The dimensionless power output versus efficiency characteristics of the endoreversible Braysson cycle can be obtained using numerical calculation.

In order to find the maximum dimensionless power output, taking the derivative of P with respect to x and setting it equal to zero ($dP/dx = 0$) gives the equation that the optimum dimensionless working fluid temperature ratio (x_{opt}) should satisfy, the maximum dimensionless power output (P_{max}) and the corresponding efficiency (η_P) as follows:

$$\frac{E_H^2 \tau \exp(x_{opt})}{[\exp(x_{opt}) + E_H - 1]^2} = \frac{U_L^2}{(U_L - C_{wf} x_{opt})^2} \tag{17}$$

$$P_{\max} = \frac{E_H \tau[\exp(x_{opt}) - 1]}{\exp(x_{opt}) + E_H - 1} - \frac{U_L x_{opt}}{U_L - C_{wf} x_{opt}} \quad (18)$$

$$\eta_P = 1 - \frac{U_L x_{opt}[\exp(x_{opt}) + E_H - 1]}{E_H \tau (U_L - C_{wf} x_{opt})[\exp(x_{opt}) - 1]} \quad (19)$$

3. Numerical examples

To see the influences of various design parameters on the power output and efficiency of the endoreversible Braysson cycle, some numerical calculations are carried out. In the analysis, $C_{wf} = 1\ \text{kW·K}^{-1}$ is assumed. Fig. 2 shows the influences of cycle heat reservoir temperature ratio τ on the dimensionless power output (P) and efficiency (η) with $E_H = 0.9$ and $U_L = 2.3\ \text{kW·K}^{-1}$. Fig. 3 shows the influences of hot-side heat exchanger effectiveness (E_H) on P and η with $\tau = 4.0$ and $U_L = 2.3\ \text{kW·K}^{-1}$. Fig. 4 shows the influences of cold-side heat exchanger heat conductance (U_L) on P and η with $\tau = 4.0$ and $E_H = 0.9$.

The results of calculations show that both P and η increase with the increases of E_H, τ and U_L. η is a monotonic decreasing function of x, while P is a parabolic-like function of x, that is there exists an optimum x (x_{opt}) corresponding to the maximum P (P_{max}). x_{opt} increases with the increases of E_H, τ and U_L. The efficiency (η_P) at maximum power output point increases with the increase of τ. η_P is not sensitive to the variations of E_H and U_L.

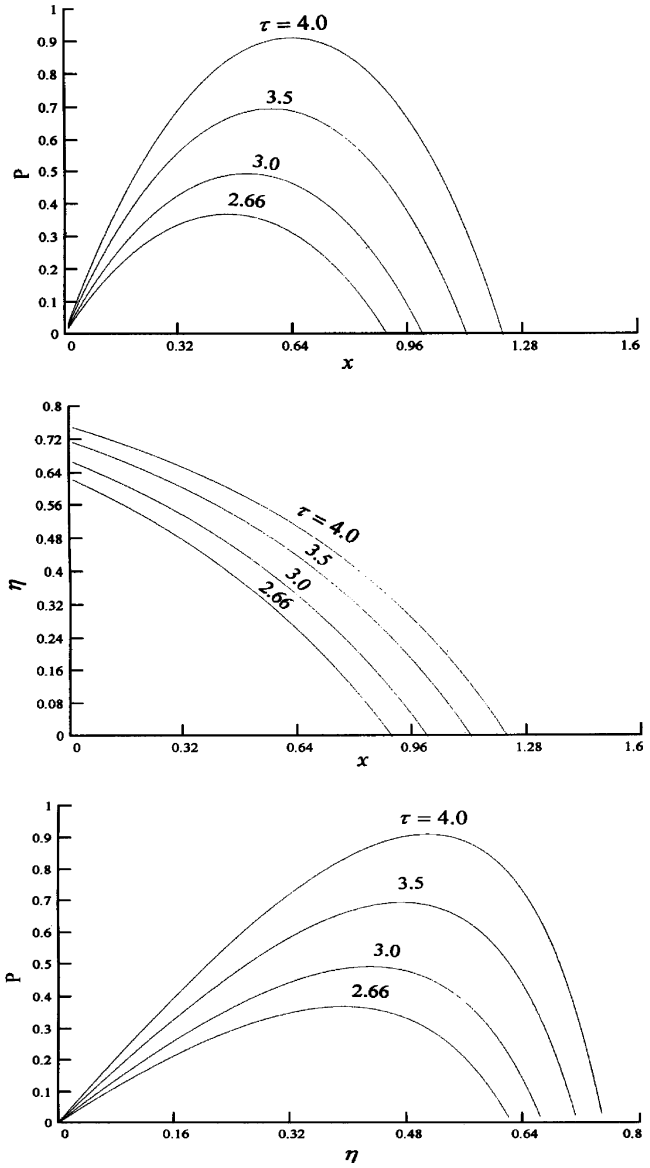

Fig. 2. Dimensionless power output (P) and efficiency (η) versus dimensionless working fluid temperature ratio (x) and heat reservoir temperature ratio (τ) with $C_{wf} = 1\ \text{kW·K}^{-1}$, $E_H = 0.9$ and $U_L = 2.3\ \text{kW·K}^{-1}$.

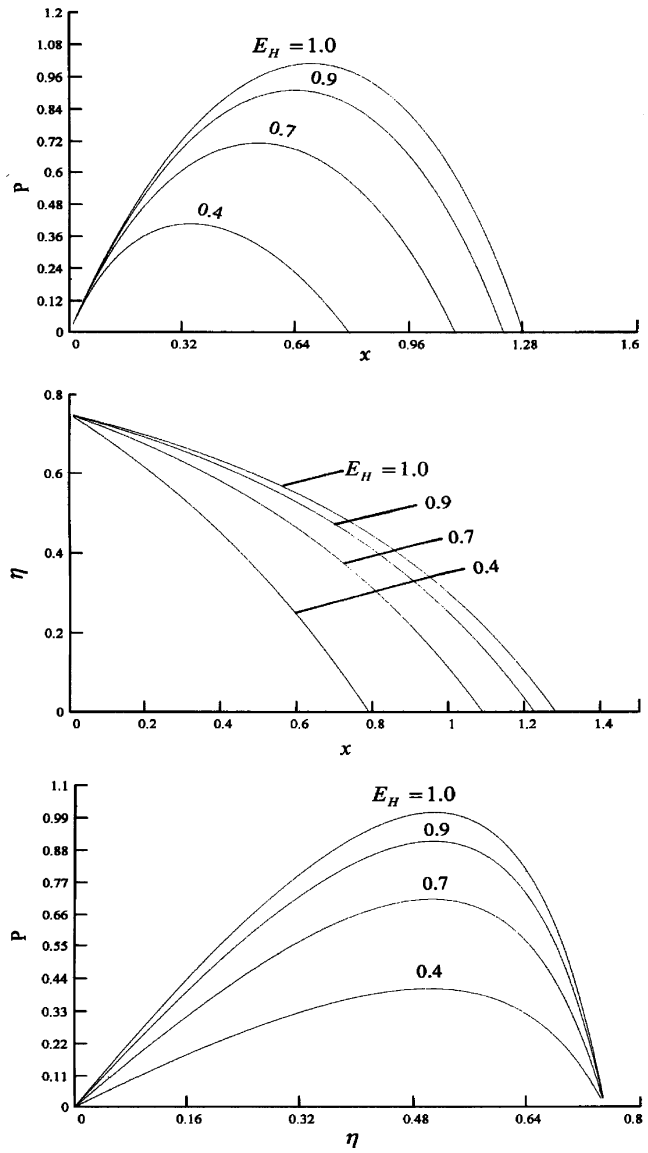

Fig. 3. Dimensionless power output (P) and efficiency (η) versus dimensionless working fluid temperature ratio (x) and hot–side heat exchanger effectiveness (E_H) with $C_{wf} = 1\ \text{kW·K}^{-1}$, $\tau = 4.0$ and $U_L = 2.3\ \text{kW·K}^{-1}$.

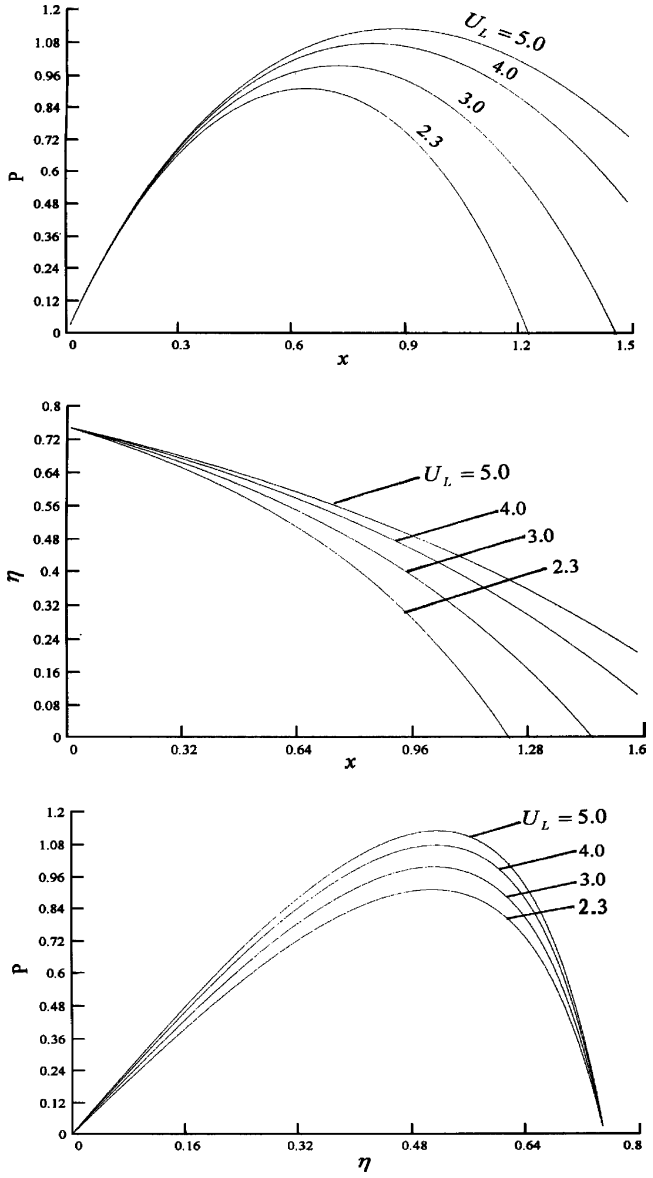

Fig. 4. Dimensionless power output (P) and efficiency (η) versus dimensionless working fluid temperature ratio (x) and cold-side heat exchanger heat conductance U_{L} with $C_{\mathrm{wf}} = 1$ kW·K^{-1}, $\tau = 4.0$ and $E_{\mathrm{H}} = 0.9$ ($U_{\mathrm{L}} = 2.3 \sim 5.0$ kW·K^{-1}).

4. Discussions

In the analysis mentioned above, E_{H}, U_{L} and C_{wf} are selected. In the case that E_{H} and U_{L} are changeable, the performance optimization can be carried out using Eqs. (15) and (16). The optimization can be performed using two different constraints alternatively. The first is to optimize the distribution of U_{H} and U_{L} with the constraint $U_{\mathrm{H}} + U_{\mathrm{L}} = U_{\mathrm{T}}$. The second is to optimize the distribution of $F_{\mathrm{H}} + F_{\mathrm{L}} = F_{\mathrm{T}}$, where F_{H}, F_{L} and F_{T} are the hot- and cold-side heat exchanger heat transfer surface areas and the total heat transfer surface area. For the fixed power output of the cycle, the former leads to the cycle with the minimum heat exchanger inventory [17], and the latter leads to the cycle with the minimum total heat transfer surface area [18]. The optimization gives the fundamental optimum power output and the optimum efficiency for the fixed x, and then gives the fundamental optimum relation between power output and efficiency. The double maximum power output can also be obtained.

5. Conclusion

Using the theory of entropy generation minimization or finite time thermodynamics, this paper analyzes the performance of a new cycle model—Braysson cycle proposed by Ref. [1]. The endoreversible assumption is used in the analysis. The further step is to analyze the irreversible cycle performance by introducing the compressor and turbine efficiencies. That analysis can provide theoretical foundation for the performance improvements of engineering cycles.

Acknowledgements

This material is based upon work supported by the National Important Fundamental Research and Development Program Project of China under the Contract No. G2000026301.

References

[1] T.H. Frost, A. Anderson, B. Agnew, A hybrid gas turbine cycle (Brayton/Ericsson): an alternative to conventional combined gas and steam turbine power plant, Proc. Instn. Mech. Engrs. 211 (1997) 121–131.
[2] B. Andresen, P. Salamon, R.S. Berry, Thermodynamics in finite time, Phys. Today (1984) 62–70.
[3] A. Bejan, Entropy generation minimization: The new thermodynamics of finite-size devices and finite time processes, J. Appl. Phys. 79 (1996) 1191–1218.
[4] L. Chen, C. Wu, F. Sun, Finite time thermodynamic optimization or entropy generation minimization of energy systems, J. Non-Equilib. Thermodyn. 24 (1999) 327–359.
[5] C. Wu, L. Chen, J. Chen (Eds.), Recent Advances in Finite Time Thermodynamics, Nova Science Publishers, New York, 1999.
[6] C. Wu, Power optimization of an endoreversible Brayton gas turbine heat engine, Energy Convers. Mgmt. 31 (1991) 561–565.
[7] O.M. Ibrahim, S.A. Klein, J.W. Mitchell, Optimum heat power cycles for specified boundary conditions, Trans. ASME J. Engrg. Gas Turbine Pow. 113 (1991) 514–521.
[8] M. Feidt, Optimization of Brayton cycle engine in contact with fluid thermal capacities, Rev. Gen. Therm. 35 (1996) 662–666.
[9] J.M.M. Roco, S. Veleasco, A. Media, A. Calvo Hernandez, Optimum performance of a regenerative Brayton thermal cycle, J. Appl. Phys. 82 (1997) 2735–2741.
[10] V. Radcenco, J.V.C. Vargas, A. Bejan, Thermodynamic optimization of a gas turbine power plant with pressure drop irreversibilities, Trans. ASME J. Energy Res. Tech. 120 (1998) 233–240.
[11] L. Chen, F. Sun, C. Wu, Performance analysis of an irreversible Brayton heat engine, J. Instit. Energy 70 (1997) 2–8.
[12] C. Wu, L. Chen, F. Sun, Performance of regenerative Brayton heat engines, Energy, Internat J. 21 (1996) 71–76.

[13] L. Chen, F. Sun, C. Wu, R.L. Kiang, Theoretical analysis of the performance of a regenerated closed Brayton cycle with internal irreversibilities, Energy Convers. Mgmt. 18 (1997) 871–877.
[14] D.A. Blank, C. Wu, Power limit of an endoreversible Ericsson cycle with regeneration, Energy Convers. Mgmt. 37 (1996) 59–66.
[15] D.A. Blank, C. Wu, Finite time power limit for solar-radiant Ericsson engines in space applications, Appl. Thermal Engrg. 18 (1998) 1347–1357.
[16] J. Chen, J.A. Schonten, The comprehensive influence of several major irreversibilities on the performance of an Ericsson heat engine, Appl. Thermal Engrg. 19 (1999) 555–564.
[17] A. Bejan, Power and refrigeration plants for minimum heat exchanger inventory, ASME Trans. J. Energy Res. Tech. 115 (1993) 148–150.
[18] B. Agnew, A. Andreson, T.H. Frost, Optimization of a steady-flow Carnot cycle with external irreversibilities for maximum specific output, Appl. Thermal Engrg. 17 (1997) 3–16.